Spectroscopic probing of acid–base properties and photocharacterization of phthalocyanines in organic solvents and polymer matrices

Sevinc Zehra Topal [a,b], Fatma Yuksel [b], Ayşe Gül Gürek [b], Kadriye Ertekin [c,*], Berrin Yenigül [a], Vefa Ahsen [b]

[a] University of Ege, Faculty of Sciences, Department of Chemistry, 35100 Bornova, Izmir, Turkey
[b] Gebze Institute of Technology, Department of Chemistry, 41400 Gebze, Kocaeli, Turkey
[c] University of Dokuz Eylul, Faculty of Arts and Sciences, Department of Chemistry, 35160 Buca, Izmir, Turkey

ABSTRACT

This work reveals spectral characterization of newly synthesized metal-free (**Pc-1**) and Zn(II) (**Pc-2**) phthalocyanines (Pcs) in conventional solvents and two solid matrices; ethyl cellulose (EC) and polyvinyl chloride (PVC). Fluorescence lifetime (τ_F) and fluorescence quantum yield values (ϕ_F) of the **Pcs** were calculated in tetrahydrofuran (THF), dimethylsulfoxide (DMSO) and solid matrices of EC and PVC. The respective protolytic forms were characterized by absorption and emission spectra as well as apparent pK_a values. The immobilized metal-free phthalocyanine exhibited strong and pH-dependent fluorescence due to a protolytic equilibrium within a large pH range yielding three different pK_a values. The Zn-II phthalocyanine also exhibited optical emission based response to proton in the pH range of 2.0–9.0. Upon exposure to proton, reversible relative signal changes for PVC-doped **Pc-1** and **Pc-2** were approximately 90 and 95%, respectively. Presence of polyvalent metal ions in test medium did not restrict the proton sensing ability of the dyes.

© 2008 Elsevier B.V. All rights reserved.

1. Introduction

Due to their promising optical and electrical properties, phthalocyanines (Pcs) are capable of forming organic conductors [1], organic light-emitting diodes [2], field effect transistors, organic photovoltaics [3], optical-chemical sensors [4–11] and tumor-localizing photosensitizers [12,13]. Excellent photostabilities, high fluorescence quantum yields (ϕ_F), long-wavelength excitation maxima and strong absorptions between 550 and 700 nm make the Pcs promising indicators in design of optical-chemical sensors. Metal-free or metal Pcs have been used as chemical-sensing agents for determination of O_2 [4], NO_2 [5–8], alcohol vapors [9] volatile organic compounds [10] and amines [11].

The phthalocyanines, along with their metal complexes, absorb light of longer wavelengths; beyond 650 nm. It should be noted that, spectral region from 600 to 1000 nm is frequently referred to as the very near-infrared region (VNIR) and is very useful for optical probing of biological material, and optical-chemical-sensing purposes [14,15]. Phthalocyanines have remarkable photostability and offer possibility to be modified by substitution and flexibility in structure, which facilitates designing of their physical, optoelectronic and chemical characteristics The offered phthalocyanines meet the requirement of exhibiting very near-infrared region (VNIR) excitation or emission wavelengths with a high sensitivity to pH in a large range.

In this work, the absorption and emission based spectral characterization of the metal-free (**Pc-1**) and Zn(II) phthalocyanine (**Pc-2**) was performed in different organic solvents, in plasticized ethyl cellulose (EC) and polyvinyl chloride (PVC). Detailed spectroscopic probing of the acid–base properties was also performed. The employed phthalocyanines; **Pc-1** and **Pc-2**; have advantages of long-wavelength excitation, high quantum yield, photostability, strong and pH-dependent fluorescence signal, high relative signal change and large dynamic working range. Their response range to proton covers the pH scale from 2.0 to 8.0. As far as we know, this is the first report of the measurement of the pH dependency for employed phthalocyanines, in solution, plasticized EC and PVC.

They are expected to be promising molecular probes for very near-infrared luminescence pH sensing studies, and to be particularly useful for applications such as labeling of biomolecules, biodistribution and tumor-photosensitizing.

2. Experimental

2.1. Reagents

Metal-free and Zn(II) Pcs were synthesized according to the method described in Ref. [16]. Chemical structures of the employed

* Corresponding author. Present address: Dokuz Eylul Universitesi Fen-Edebiyat Fakultesi, Kimya Bolumu 35160, Tinaztepe Buca, Izmir, Turkey.
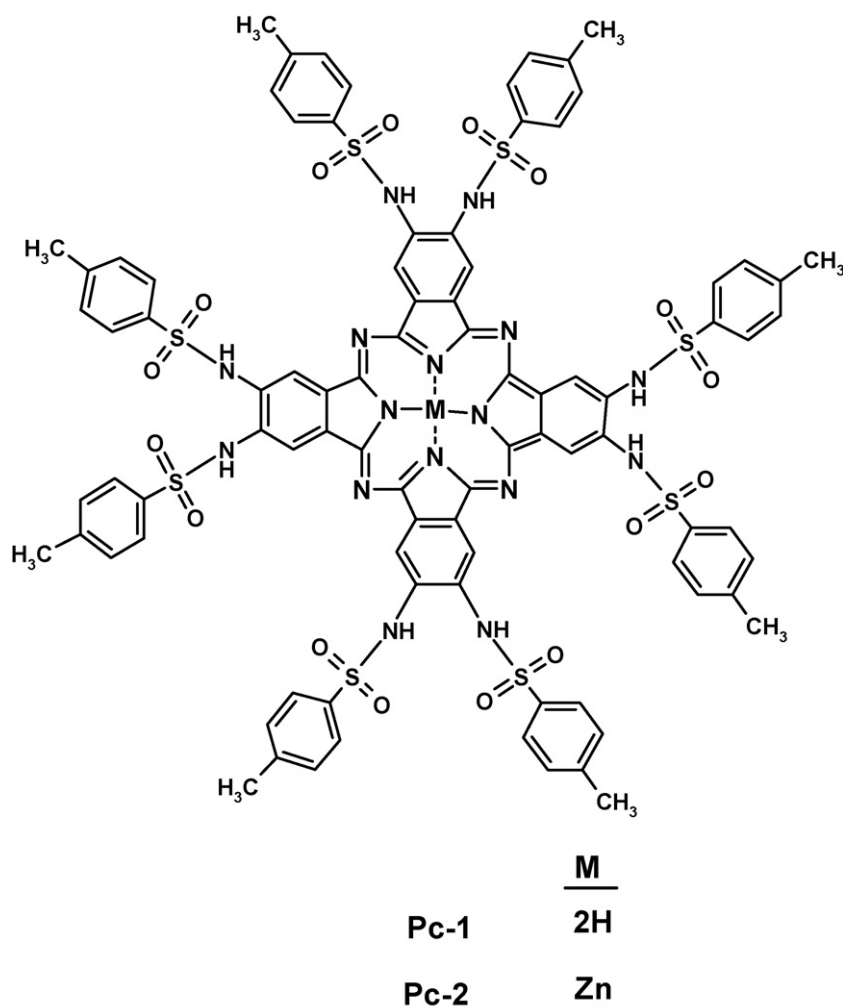 *E-mail address:* kadriye.ertekin@deu.edu.tr (K. Ertekin).

	M
Pc-1	**2H**
Pc-2	**Zn**

Fig. 1. Chemical structures of the metal-free (**Pc-1**) and Zn(II) (**Pc-2**) octa-(tosylamido) phthalocyanines.

molecules were shown in Fig. 1. The polymer membrane components, polyvinyl chloride (PVC) (high molecular weight), ethyl cellulose (EC) and the plasticizer, bis-(2-ethylhexyl) phthalate (DOP) were obtained from Merck and Fluka. Potassium tetrakis-(4-chlorophenyl) borate (KTClPB) was from Aldrich. Chloroform ($CHCl_3$), tetrahydrofuran (THF), and dimethylsulfoxide (DMSO) were of analytical grade. Solvents for the spectroscopic studies used without further purification. Tetrabutylammonium hydroxide (TBAOH, 0.1 M, in isopropanol), trifluoroacetic acid and perchloric acid ($HClO_4$) were purchased from Merck. Buffer solutions were prepared with disodium hydrogen phosphate/sodium hydroxide for pH 12.0, sodium dihydrogen phosphate/sodium hydroxide for pH 7.0, and phosphoric acid/sodium hydroxide for pH 2.0. Millipore pure water was used throughout the studies.

2.2. Instrumentation

Absorption spectra were recorded using Shimadzu 2101 UV–visible spectrophotometer. Steady-state and fiber optic fluorescence measurements were recorded by using Varian Cary Eclipse spectrofluorometer. The wavelength resolution of the fluorescence spectrometer and UV–vis spectrophotometer used to measure spectra are <1.5 nm and 0.01 nm respectively. A home-made black Teflon flow-cell and a bifurcated fiber coupler were used for pH-sensing measurements. The excitation light was carried to the cell through one arm of the bifurcated fiber and the emission light

was acquired through the other. The tip of bifurcated fiber optic probe was interfaced with the sensing membrane fixed on the top of the flow chamber as shown in Ref. [17]. The sample or buffer solution was driven into the 300 μL flow-cell by a peristaltic pump (Four channels Ismatec Reglo Analog) at a flow rate of 2.2 mL min^{-1}. Tygon tubing of 2.06 mm inner diameter was used with the peristaltic pump. pH of the solutions was measured with a digital pH meter (WTW), which was calibrated with standard buffers of pH 4.0, 7.0 and 10.0. All measurements were performed at room temperature (25 °C) and under atmospheric pressure.

2.3. Preparation of sensing membrane

The PVC based polymer membrane was prepared to contain 120 mg of PVC, 240 mg of plasticizer (DOP), 1.5 mg of **Pc-1** or **Pc-2**, and 3.5 mg of potassium tetrakis-(4-chlorophenyl) borate and 1.5 mL of THF. The EC based polymer membrane was prepared to contain 100 mg of EC, 200 mg of plasticizer (DOP), 1.5 mg of **Pc-1** or **Pc-2**, 3.5 mg of potassium tetrakis-(4-chlorophenyl) borate and 1.5 mL of THF.

The resulting cocktails were spread onto a 125 μm polyester support (Mylar^{TM}) in order to obtain sensor films. The films were dried in ambient air of laboratory. Then thin films of approximately 5 μm were obtained on the Mylar support. The polyester support was fully transparent and exhibited good adhesion to PVC and EC. Each sensing film was cut to 1.2 cm × 3.0 cm size, fixed diagonally into
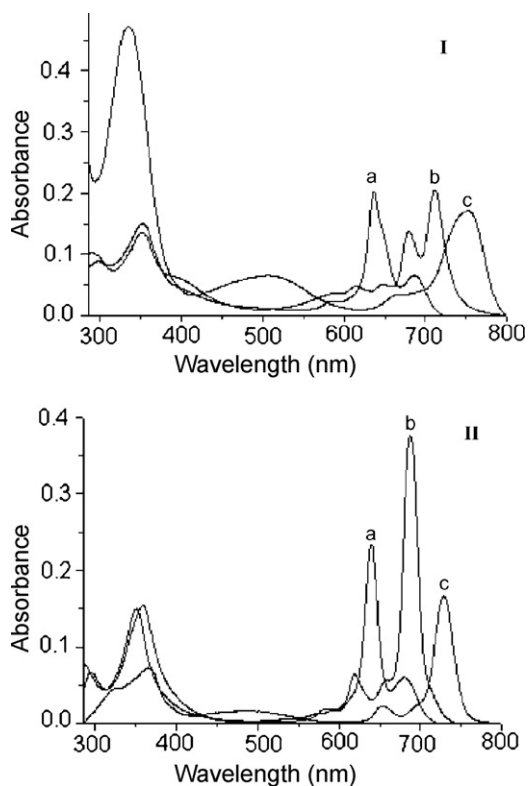
Fig. 2. Absorbance spectra of molecules, (I) **Pc-1** and (II) **Pc-2** in different solvents: (a) chloroform, (b) THF and (c) DMSO.

the sample cuvette for the steady-state measurements. For flow through measurements, the sensor films of 30 mm diameter were cut and placed into the flow-cell containing 300 µL buffer solutions.

3. Results and discussion

3.1. Absorption based spectral characterization

Spectral characterization of metal-free and Zn(II) Pcs was performed with recording absorption, excitation and emission spectra in the solvents of $CHCl_3$, THF, and DMSO and in solid matrices of EC and PVC. Fig. 2 shows gathered absorption spectra of **Pc-1** and **Pc-2** in the employed solvents. UV–vis spectroscopy related data; absorption maxima; λ_{Abs} and molar extinction coefficients of the Pcs were shown in Table 1.

The employed Pcs exhibited typical electronic spectra with strong absorption bands: an ultraviolet Soret (B) band around 350 nm and a visible Q band around 700 nm. In case of metal-free phthalocyanine, the Q band split into two which arises from its lower symmetry (D_{2h}) compared with that of metal-

phthalocyanine (D_{4h}). The **Pc-1** exhibited the typical split Q bands at 681 and 710 nm in THF. However, the **Pc-1** yielded two Q bands in chloroform; a monomeric Q band around 680 nm and a blue shifted dimeric band around 640 nm; corresponding to protonated species. The single Q band of **Pc-1** in DMSO was shifted to red 30 and 103 nm with respect to the intense component of Q band in THF and $CHCl_3$, respectively. The non-split Q band of **Pc-1** observed in DMSO can be attributed to the deprotonation of the central pyrolle nitrogens due to the basicity of the solvent. The 103 nm of red shift observed in DMSO with respect $CHCl_3$ also arises from deprotonation of octa-tosylamido moiety of the phthalocyanines. The spectral shifts seen for **Pc-2** in the employed solvents were parallel to the shifts observed for **Pc-1** and can be explained in the same way (see Fig. 2, Table 1).

All these spectral diversities observed in DMSO can be attributed to the solvatochromism and basicity of the solvent [16].

Absorption spectra of the immobilized **Pc-1** and **Pc-2** in EC and PVC were also investigated. Split Q bands of **Pc-1** and **Pc-2** appeared at 688 and 630 nm, and, 686 and 625 nm in PVC, respectively. However, different results were observed in EC; the split Q bands of **Pc-1** and **Pc-2** disappeared and two single bands appeared at 707 and 692 nm, respectively. Upon immobilization in PVC, while the intensity of monomeric Q band decreasing, dimeric Q band increased and became more effective. Among the employed media, the highest molar extinction coefficients were observed in THF and EC (see Table 1).

3.2. Emission based studies

Four pyrrole rings of the phthalocyanines corresponding macro cycle have fully conjugated aromatic π-electrons which are responsible from intense fluorescence of the Pcs. Table 2 reveals the excitation and emission spectra related characteristics (emission maxima, excitation maxima, Stoke's shift, fluorescence quantum yield and fluorescence lifetime) of **Pc-1** and **Pc-2** in the employed solvents and solid matrices. In all cases, dyes were excited around 665–720 nm and emission spectra were recorded. In agreement with literature [18], metal-free Pc (**Pc-1**) exhibited long-wavelength emission maxima in the solvents and solid films with respect to corresponding Zn(II) Pc (**Pc-2**) which can be attributed to the charge transfer transitions between the ring and the metal cation.

It should be noted that, preferred excitation wavelengths for biological fluids, including urine, blood, serum or plasma is 600 nm or greater. The **Pc-1** and **Pc-2** excited at 679 and 665 nm in THF and 682 and 665 in PVC which are proper for test-kit applications for blood and serum.

In all of the employed matrices, the Stoke's shift values of the phthalocyanines calculated from spectral data were high enough for spectral resolution. Stoke's shift is important for fluorescence and optical-sensing studies because the high Stoke's shift value allows the emitted fluorescence photons to be easily distinguished from the excitation photons, leading to the possibility of very low

Table 1
UV–vis spectrum related data of **Pc-1** and **Pc-2** in the solvents of $CHCl_3$, THF, DMSO and in solid matrices of EC and PVC.

Compound	Solvent/matrix	λ_{abs}^1	λ_{abs}^2	λ_{abs}^3	$\varepsilon_{max}(\lambda_{abs}^1)(\times10^4)$	$\varepsilon_{max}(\lambda_{abs}^2)(\times10^4)$	$\varepsilon_{max}(\lambda_{abs}^3)(\times10^4)$
Pc-1	$CHCl_3$	351	637	686	9.5	13.9	5.3
	THF	352	648	681, 710	1.0	4.1	16.2, 16.9
	DMSO	354	534	740	8.2	3.4	11.9
	EC	348	503	707	7.7	2.5	7.9
	PVC	357	639	688	11.0	12.2	5.1
Pc-2	$CHCl_3$	351	640	682	7.4	12.7	3.8
	THF	358	659	687	8.9	7.2	22.8
	DMSO	364	523	721	6.8	1.5	10.2
	EC	355	640	692	3.3	4.1	16.9
	PVC	354	641	686	11.9	15.5	5.8

Table 2
Fluorescence spectra related data of **Pc-1** and **Pc-2** in the solvents of CHCl$_3$, THF, DMSO and in solid matrices of EC and PVC (λ_{max}^{em}: maximum emission wavelength in nm; λ^{ex}: maximum excitation wavelength in nm; $\Delta\lambda_{ST}$: Stoke's shift in nm; ϕ_F: quantum yield and τ_F: fluorescence lifetime in ns).

Compound	Solvent/matrix	λ_{max}^{em}	λ^{ex}	ϕ_F	τ_F	$\Delta\lambda_{ST}$
	CHCl$_3$	715	675	Very low	–	40
	THF	715	679	0.33	1.23	36
Pc-1	DMSO	780	720	0.03	0.07	60
	EC	718	683	0.23	0.33	35
	PVC	718	682	0.03	0.06	36
	CHCl$_3$	707	660	Very low	–	47
	THF	694	665	0.25	1.44	29
	DMSO	748	680	0.15	0.71	68
Pc-2	EC	698	665	0.15	0.41	33
		742 (acidic)	665	0.13	0.36	77
	PVC	698	665	Very low		
		746 (acidic)	665	0.28	5.54	33

background signals. All of the Pcs, exhibited Stoke's shifts exceeding the minimum of 30 nm recommended for easy visualization and sensitive detection in most of the employed media (see Table 2).

3.3. Fluorescence quantum yield and lifetime calculations

Fluorescence quantum yields (ϕ_F) of the **Pc-1** and **Pc-2** were calculated employing the comparative William's method [19], which involves the use of well-characterized standards with known ϕ_F values. For this purpose, the UV–vis absorbance and corrected emission spectra of different concentrations of reference standard, the **Pc-1** and **Pc-2** were recorded respectively. Unsubstituted Zn-Pc was used as reference standard whose fluorescence quantum yield is 0.18 in DMSO. Integrated fluorescence intensities were plotted versus absorbance for the reference standard, **Pc-1** and **Pc-2**. Slopes of the plots were proportional to the quantity of the quantum yield of the studied molecules. The quantum yield values were corrected by multiplying with a correction factor of $(1.0\phi_F/0.18)$ in order to convert to absolute value considering the ϕ_F of the standard 1.0.

Fluorescence quantum yields (ϕ_F) were calculated according to the following equation where ST and X denote standard and sample, respectively. *Grad* is the gradient of the plot and *n* is the refractive index of the solvent or polymer matrix material [19].

$$\phi_F = \phi_{ST} \left(\frac{Grad_X}{Grad_{ST}} \right) \left(\frac{n_X^2}{n_{ST}^2} \right)$$

The **Pc-1** and **Pc-2** exhibited quite high quantum yields in THF, EC and PVC in their neutral form. The ϕ_F values of **Pc-1** and **Pc-2** were found to be 0.33 and 0.25 in THF, respectively. The quantum yield value of **Pc-2** in PVC in an acidic environment was found to be 0.28 at 746 nm which is 5.5-fold of ϕ_F of **Pc-2** in EC. Calculated quantum yield values reveal that the **Pc-2** dye fluoresce better in immobilized PVC matrix in acidic environments than that of other employed media (see Table 2).

Fluorescence lifetimes (τ_F) were determined using Photochem-CAD program which uses the Strickler–Berg equation [20]. Fluorescence lifetimes of the **Pc-1** and **Pc-2** were determined as 1.23 and 1.44 nanoseconds in THF, respectively (see Table 2). The longest fluorescence lifetimes were measured in EC and acidic PVC for **Pc-2**.

3.4. Spectroscopic probing of acid–base properties of **Pc-1** and **Pc-2** in THF

The knowledge of acidity constant (pK_a) is of fundamental importance in order to provide information on chemical reactivity range of the indicator dyes. For this reason, the absorption and emission based pH dependencies of **Pc-1** and **Pc-2** were investigated in THF. pH-dependent absorption spectra of **Pc-1** and **Pc-2** in THF were given in Fig. 3. The **Pc-1** exhibited a response to proton ions in direction of signal decrease from pH 3.4 to 5.5. From pH 5.5 to 13.6, direction of the signal inversed and split Q band of the **Pc-1** was disappeared. With increasing pH, Q band spectra of **Pc-1** were also shifted to red. The **Pc-2** in THF exhibited similar spectral response to proton ions (see Fig. 3II).

pH-dependent emission spectra of **Pc-1** and **Pc-2** in THF were given Fig. 4. The emission peak of **Pc-1** at 715 nm decreased upon
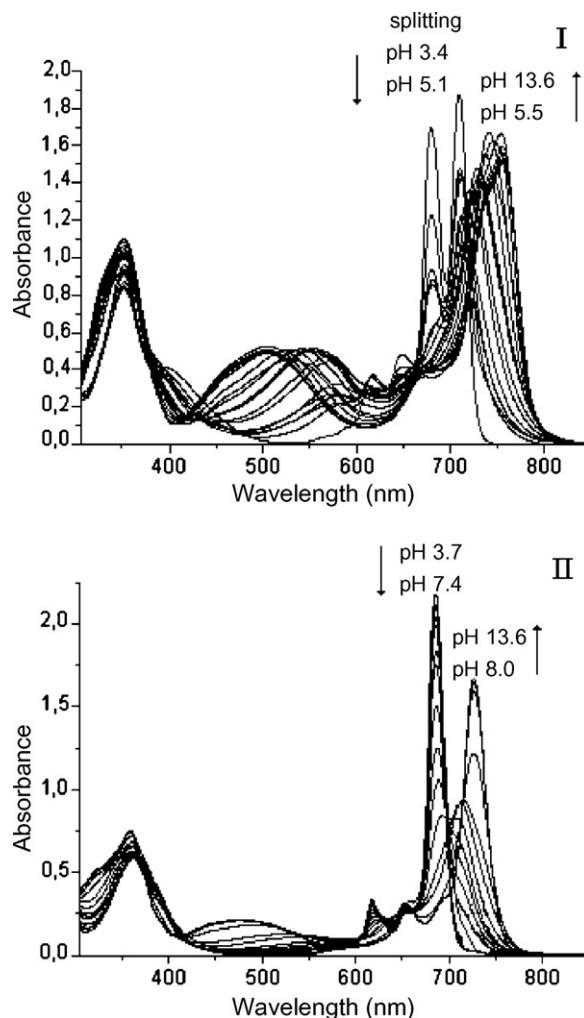

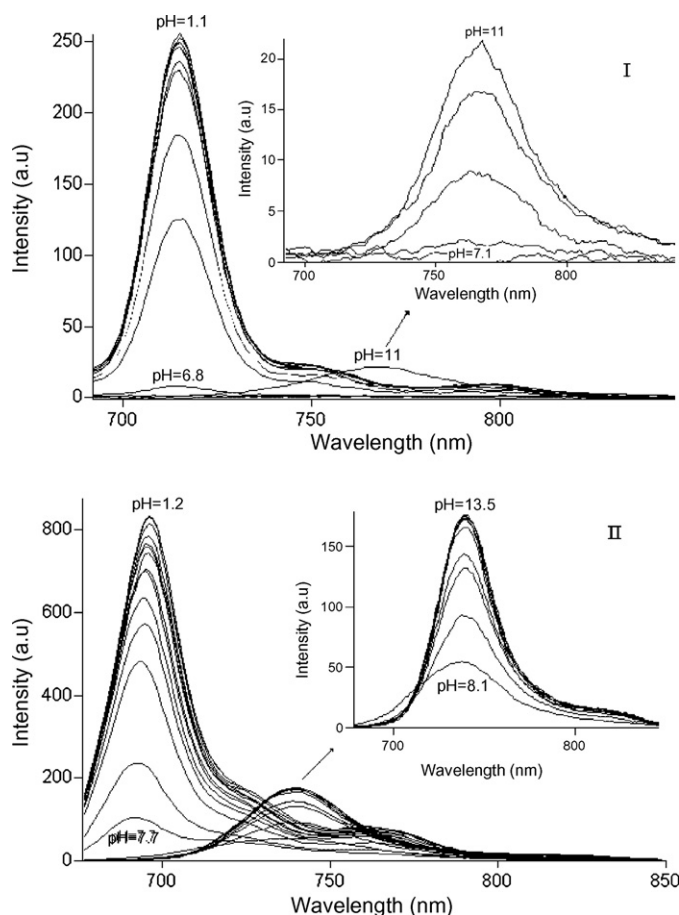**Fig. 3.** (I) pH-dependent absorption spectra of **Pc-1** and (II) **Pc-2** in THF.

Fig. 4. pH-dependent fluorescence emission spectra of **Pc-1** and **Pc-2** in THF. (I) Fluorescence spectra between pH 1.1 and 6.8 (pH 1.1, 1.9, 3.0, 4.1, 6.0, 6.4, 6.6, 6.7, 6.8) at 715 nm. Inset spectra: between pH 7.1 and 11.0 (pH 7.1, 7.9, 8.9, 9.6, 11.0) at 767 nm and (II) Fluorescence spectra between pH 1.2 and 7.7 (pH 1.2, 2.4, 3.8, 4.2, 5.0, 5.6, 6.6, 6.7, 6.8, 7.0, 7.7) at 696 nm. Inset spectra: between pH 8.1 and 13.5 (pH 8.1, 8.7, 9.3, 9.9, 10.7, 11.0, 11.4, 12.5, 13.5) at 740 nm.

exposure to proton ions between pH 1.1 and 6.8. The spectral response to proton in the pH range of 7.1–11.6 observed at 767 nm was negligible (see inset of Fig. 4). From the inflection point of the dissociation curve, the pK_a value of the **Pc-1** was determined as $pK_a = 6.9$. Similarly the **Pc-2** exhibited a decreasing signal response to proton ions in the pH range of 1.2–7.7 at 696 nm. The pH-dependent response observed at 740 nm between pH 8.1 and 13.5 was omitted (see inset of Fig. 4). The pK_a value of the **Pc-2** in THF was found to be 6.8 from the inflection point of dissociation curve.
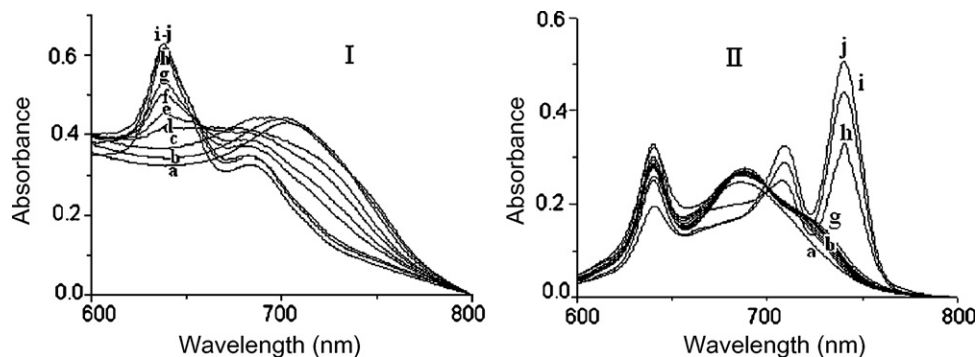
Fig. 6. (I) Fluorescence excitation and emission spectra of the **Pc-1** in PVC films at different pH values: (a) 14.0–9.0, (b) 8.5, (c) 8.0, (d) 7.5, (e) 7.0, (f) 6.5–5.0, (g) 4.5, (h) 4.0, (i) 3.5, (j) 3.0–1.0 and (II) emission based sigmoidal response of **Pc-1** to pH.

3.5. Spectroscopic probing of acid–base properties of *Pc-1* and *Pc-2* in PVC

The absorption behavior of PVC-doped phthalocyanines exhibited diversities with respect to the absorption spectrum recorded in THF. Absorption based pH response of PVC-doped **Pc-1** and **Pc-2** were shown in Fig. 5. While the immobilized **Pc-1** exhibiting an isobestic point at 660 nm, the **Pc-2** yielded a new absorption peak at 740 nm in acidic environments. pH-dependent excitation and emission spectra of **Pc-1** exhibited an increasing response to proton from pH 12.0 to 1.0. The excitation–emission spectra and related dissociation curves of **Pc-1** and **Pc-2** were shown in Figs. 6 and 7, respectively. From Fig. 6, it can be concluded that **Pc-1** exhibited two distinct and one weak inflection points corresponding to the pK_a values of 3.5, 7.2 and 8.4. Therefore, PVC-doped **Pc-1** dye can be effectively used for the pH sensing purposes in the pH range of 2.5–4.5 and 6.2–8.2.

Fig. 5. Absorption based response of (I) **Pc-1** and (II) **Pc-2** in PVC film at different pH values: (a) 10.0, (b) 9.0, (c) 8.0, (d) 7.0, (e) 6.0, (f) 5.0, (g) 4.0, (h) 3.0, (i) 2.0 and (j) 1.0.
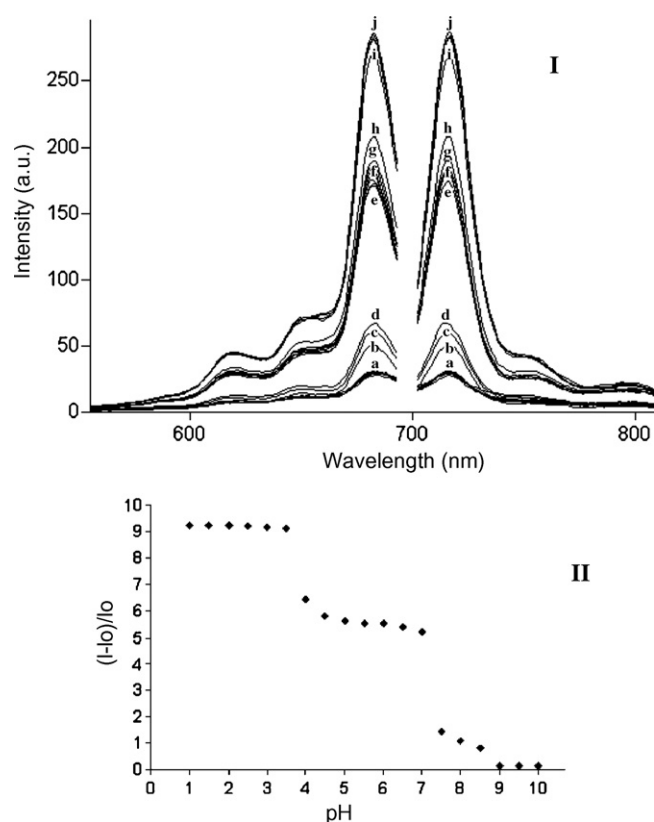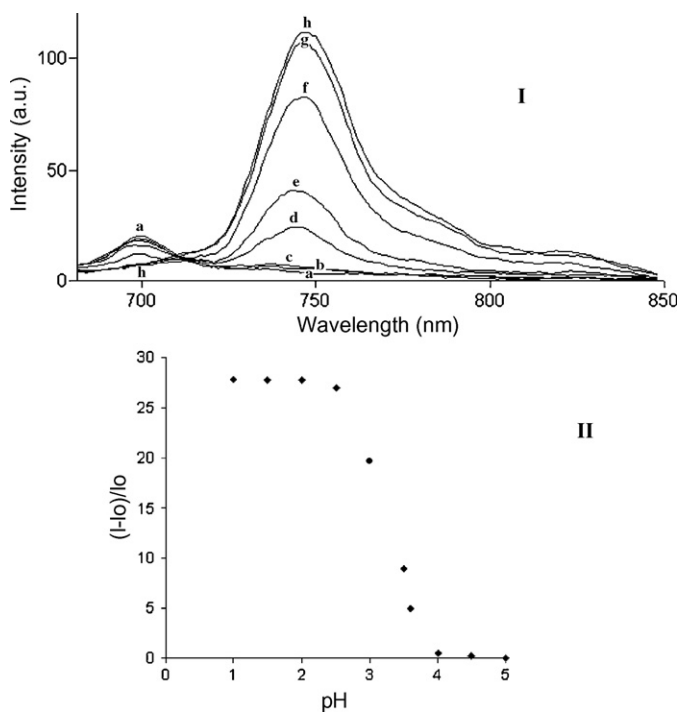
Fig. 7. (I) Fluorescence emission spectra of the molecule, **Pc-2** in PVC films at different pH values: (a) 12.0–5.0, (b) 4.5, (c) 4.0, (d) 3.6, (e) 3.5, (f) 3.0, (g) 2.5 and (h) 2.0–1.0 and (II) emission based sigmoidal response of **Pc-2** to pH.

Fig. 7 reveals emission based spectra of PVC-doped **Pc-2**. pH dependency of **Pc-2** was investigated at 746 nm in pH range of 12.0–1.0. The analytical signal was the increasing emission intensity between pH 2.0 and 4.0. In contrast to **Pc-1**, the pK_a value of **Pc-2** in PVC was found to be 3.3 from the inflection point of the dissociation curve (see Fig. 7II).

The immobilized **Pc-1** and **Pc-2** reversibly responded to H$^+$ ions in PVC. Protonation reaction was faster than deprotonation process for both of the molecules.

3.6. pK$_a$ calculations of Pc-1 and Pc-2 in EC

pH dependency of metal-free and Zn(II) phthalocyanines in EC was very similar to the pH response observed in THF. At neutral pH values, the absorption spectrum exhibited the typical splitting Q band structure of low symmetry species, attributable to the neutral PcH$_2$ possessing D$_{2h}$ symmetry. The splitting of the Q band for **Pc-1** disappeared depending on degree of the deprotonation of pyrrole nitrogens (see Fig. 8).

Fig. 9. (I) Fluorescence excitation and emission spectra of the molecule, **Pc-1** in EC films at different pH: (a) 12.0, (b) 10.5, (c) 9.0, (d) 8.0, (e) 7.0, (f) 6.0, (g) 5.0, (h) 4.0, (i) 3.0 and (j) 2.0–1.0 and (II) emission based sigmoidal response of **Pc-1** to pH.

Fluorescence spectra of **Pc-1** in EC between pH 1.0 and 11.0 and emission based sigmoidal response (pH versus $(I - I_o)/I_o$) were shown in Fig. 9I and II, respectively. pK_a values for EC doped **Pc-1** were determined as pK_{a1} = 3.6, pK_{a2} = 6.5 and pK_{a3} = 8.7 from the inflection points.

Fluorescence spectra of **Pc-2** in EC between pH 1.0 and 11.0 and related emission based sigmoidal response were similar to the response of **Pc-1**. The pK_a values of **Pc-2** were found to be pK_{a1} = 2.5 (slight), pK_{a2} = 5.6 and pK_{a3} = 9.0 from the inflection points. The **Pc-1** and **Pc-2** reversibly responded to H$^+$ ions in EC. The EC doped **Pc-1** and **Pc-2** dyes can be effectively used for the pH sensing purposes in the pH range of 3.0–9.0.
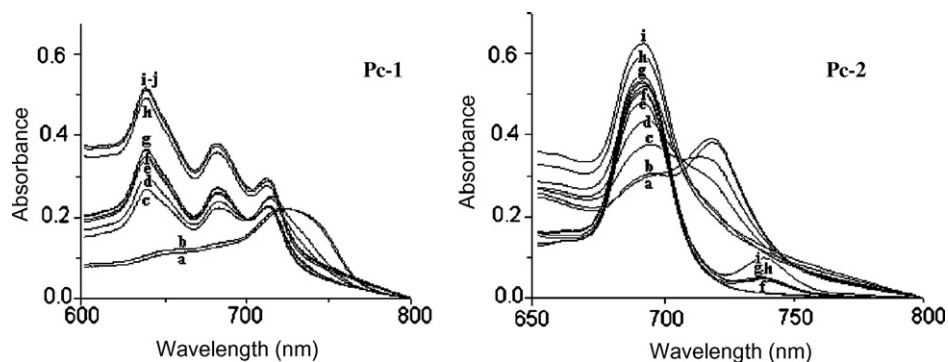

Fig. 8. Absorption based responses of the **Pc-1** and **Pc-2** to pH in EC films. **Pc-1**: (a) pH 12.0, (b) 10.5, (c) 9.0, (d) 8.0, (e) 7.0, (f) 6.0, (g) 5.0, (h) 4.0, (i) 3.0 and (j) 2.0–1.0. **Pc-2**: (a) pH 12.0, (b) 10.5, (c) 9.0, (d) 8.0, (e) 7.0, (f) 6.0–4.0, (g) 3.0, (h) 2.0 and (i) 1.0.
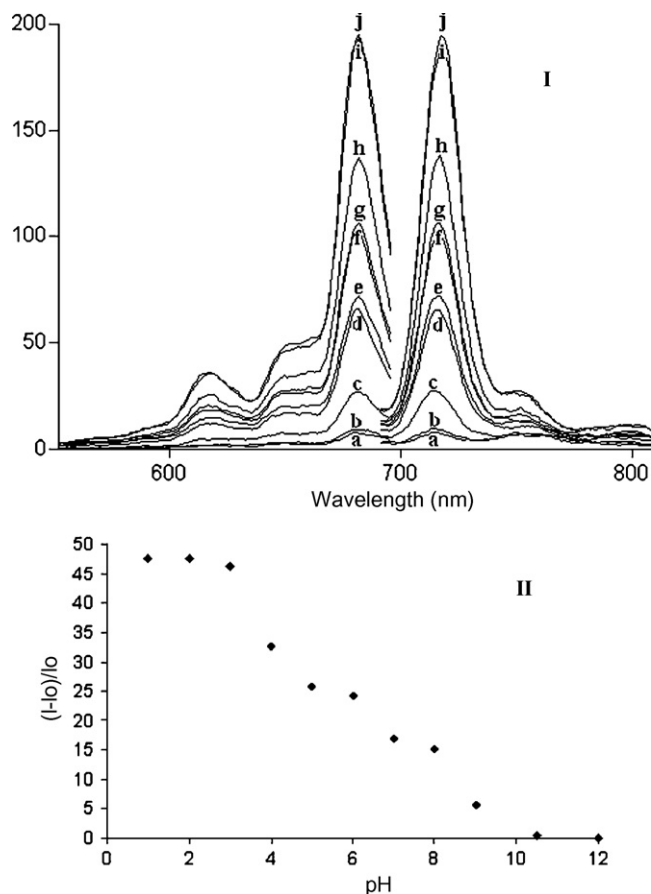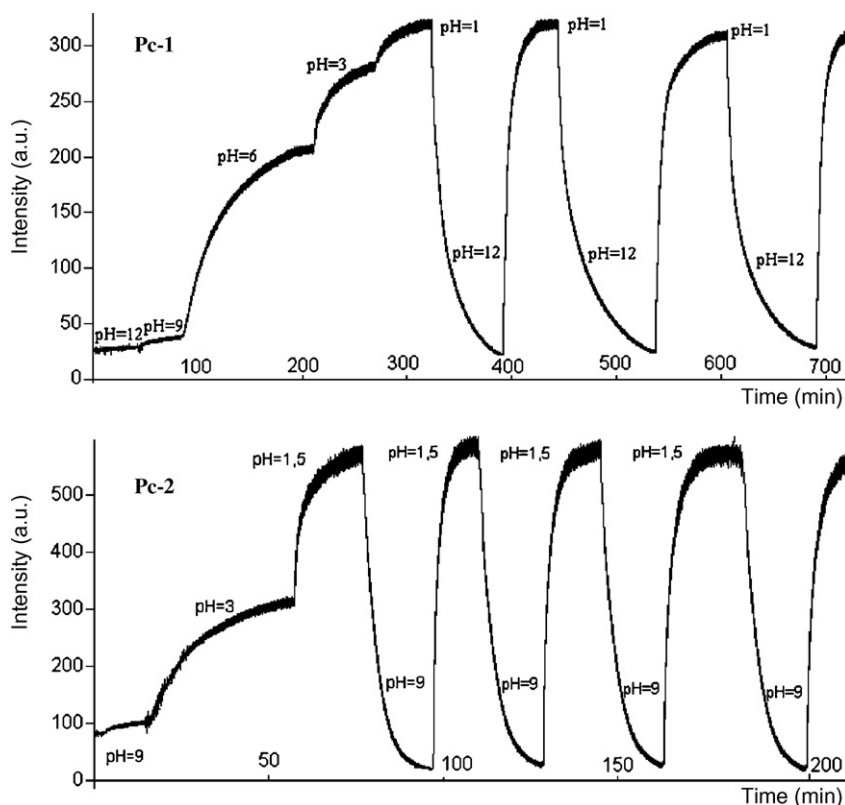
Fig. 10. Response curve and regeneration performance of PVC-doped **Pc-1** and **Pc-2**.

The Pc dyes exhibited three different distinct inflection points and corresponding pK_a values when doped into PVC or EC together with lipophilic anionic additive; potassium tetrakis-(4-chlorophenyl) borate. Incorporation of stoichiometric amount of anionic sites such as KTClPB with polymer is essential for a functional ion sensing for proper uptake of protons into the membrane. The formation of three different pK_a values for **Pc-1** in EC can be attributed to the successive deprotonation of inner pyrolle nitrogens, deprotonation of the outset octa-tosylamido nitrogens and then protonation of the external nitrogens. On the other hand, acidity of two octa-tosylamido nitrogens linked to a benzene ring are probably different. Nevertheless deprotonation of inner pyrolle nitrogens and deprotonation belong to one of the octa-tosylamido nitrogens are likely very close so one pK_a value found belong to these.

The KTClPB containing thin film forms of plasticized membranes allow ion transport through the membrane and provide enough accessibility for proton ions.

3.7. Interpretation of acid–base behavior of the phthalocyanines

The metal-free phthalocyanine; **Pc-1** contains four pyrolle nitrogens, all of which are theoretically capable of undergoing protonation/deprotonation reactions (see Fig. 1). The protonation or deprotonation state of the pyrrole-imine moiety affects the absorption spectrum, namely the number, location and strength of the Q bands. This can be attributed to the partial charge transfer from the nitrogen atoms to the phthalocyanine π-electron system under formation of a stabilized cation which can be represented with lots of different resonance structures. In our experiments, Q band of **Pc-1** was observed single in alkaline solutions, indicative of the D_{4h} symmetry of the fully deprotonated species Pc^{2-}, this change is attributed to reversible deprotonation of the central imine groups [21]. At low pH values, the spectrum exhibits the typical split Q band

structure of low symmetry species, attributable to the neutral H_2Pc possessing D_{2h} symmetry. This behavior can also be explained on the basis of the pyrrole nitrogen atoms being very acidic, because of the electron-pulling effect of the tosyl groups.

As special for **Pc-2**, it is well known for zinc phthalocyanines, protonation of external nitrogen in acidic medium lead to lowering of symmetry, resulting in splitting and bathochromic shift of the Q band (see Fig. 5).

Studies by our group showed that the stepwise protonation of the deprotonated both phthalocyanines in basic medium resulted with successive blue shifts of the Q band, with the protonated species absorbing about 60 nm of the red of both unprotonated **Pcs** (see Fig. 3). These protonated species were fluorescent and their emission spectra exhibited similar blue shifts extending to 50–60 nm (see Fig. 4).

Both of the dyes discussed above contain available active centers for proton attacks and are appropriate for using as pH probes. When they are immobilized in EC and PVC along with anionic additive; potassium tetrakis-(4-chlorophenyl) borate; **Pc-1** and **Pc-2** become H^+ selective molecular probes. In these systems, H^+ ions are selectively extracted into the optode membrane by the anionic additive meanwhile potassium ions diffuse from the membrane into the aqueous phase due to the mechanism of ion-exchange.

3.8. Performance studies of sensor films

The response performances of the pH sensor slides were evaluated in terms of reproducibility, reversibility and response time. The response characteristics of **Pc-1** and **Pc-2** were investigated with fiber optic probe in a flow system. The fluorescence intensity change upon switching the pH from 12.0 to 1.0 was recorded for PVC-doped **Pc-1** and **Pc-2** (see Fig. 10). Sensor membranes of **Pc-1** and **Pc-2** were found to reach 90% of the signal intensity change (τ_{90}) in 21.6 ± 1.5 and 13.9 ± 1.6 min respectively (n = 10 cycles).
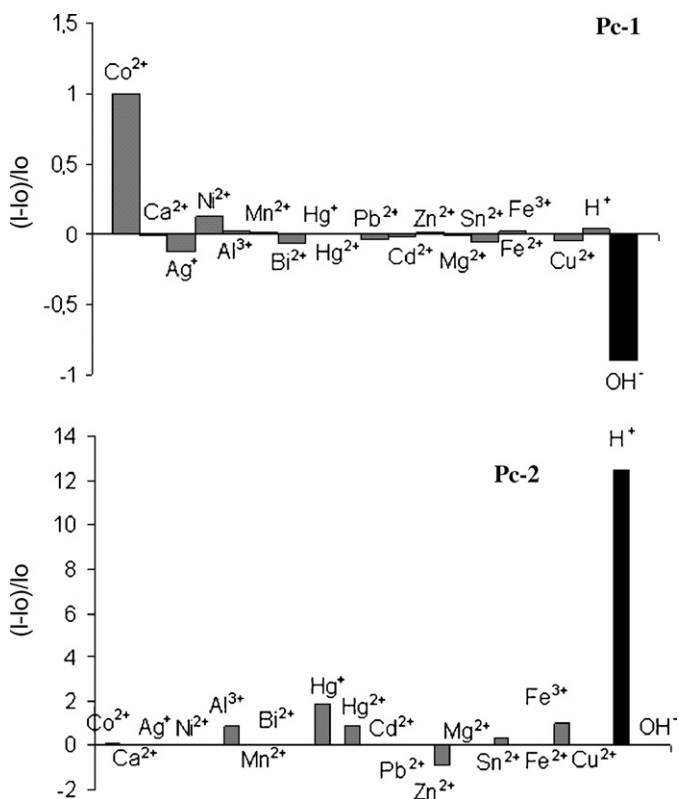
Fig. 11. Metal ion responses of PVC-doped **Pc-1** (at 715 nm) and **Pc-2** (at 746 nm), respectively. Results were plotted as relative fluorescence changes $(I - I_0)/I_0$, where I was the fluorescence intensity of the sensor membrane after exposure to ion-containing solutions and I_0 is the fluorescence intensity of the sensor slide in ion-free buffer solution.

The average regeneration times for **Pc-1** and **Pc-2** were found to be 18.9 ± 2.1 and 13.4 ± 1.4 min. Regeneration recoveries of **Pc-1** and Pc-2 were approximately 100% even after 10 cycles.

The reported response and recovery times include the dead volume of the tubings, rather than the true response time of the sensing composition. Additionally, the response time can be improved by adjusting the film thickness of sensor slides and the flow rate of the buffer solutions. In our case, average film thickness was found to be 5 μm. The film thickness can be reduced and shorter response times can be reached.

All these results for **Pc-1** and **Pc-2** imply that reproducibility, reversibility and relative signal changes of the proposed sensor for pH measurements are satisfactory. In EC matrix based studies very similar reproducibility performance was obtained for both dyes. In all of the employed media; in THF, PVC and EC; the protonation–deprotonation behavior of the Phthalocyanine dyes was reversible.

3.9. Effect of the ionic strength and cross-sensitivity to metal cations

The effect of ionic strength on the sensor membranes of **Pc-1** and **Pc-2** was investigated using phosphate buffer solutions of pH 5.0 whose ionic strengths were adjusted to 0.1 or $1.0 \, \mathrm{mol \, L^{-1}}$ with NaCl. The employed range covers most of the clinical and biotechnical applications. Fluorescence intensity of PVC-doped **Pc-1** and **Pc-2** did not give any significant change with increasing ionic strength up to $1.0 \, \mathrm{mol \, L^{-1}}$.

The interference effects of a number of common species on the fluorescence determination of pH were also investigated by exposure to 10^{-3} M solutions of Zn^{2+}, Hg^+, Sn^{2+} Ca^{2+}, Bi^{2+}, Na^+, Ni^{2+},

Co^{2+}, Cu^{2+}, Pb^{2+}, Al^{3+}, Cr^{3+}, Mn^{2+}, K^+, Fe^{2+} and Fe^{3+} for **Pc-1** and **Pc-2**. Fig. 11 reveals fluorescence emission based response of **Pc-1** and **Pc-2** to the metal cations. The interference experiments were performed in 10^{-2} M acetic acid buffered solutions at pH 5.0. Except that of Co^{2+}, for common polyvalent metal ions, relative errors of less than 5% were obtained. This was considered tolerable. The **Pc-1** and **Pc-2** in PVC exhibited good selectivity towards hydrogen ions with respect to other co-existing interferences, which made it feasible for practical applications. It should be noted that, spectroscopic responses to metal ions are dependent on many factors, including pH, temperature, viscosity, and the presence of other ions. At very low pH values, the alkali metal cations Na^+ and K^+ act as H^+ ions and disturbs the signal of **Pc-1** and **Pc-2** by taking place of proton. The relative response of phthalocyanines to acetate and chloride were very slight, <0.5% at neutral pH's.

4. Conclusion

The advantages of working with fluorophores emitting beyond 650 nm are well known. We believe that the offered phthalocyanines will be potential candidates for practical applications like the development of a photodynamic therapy agent with increased sensitivity and selectivity. The knowledge of pH-dependent spectral changes of the metal-free and metal-phthalocyanines both in solution phase and in immobilized form is of fundamental importance in order to provide information on their chemical reactivity range. Here, we have reported pH dependency and photopysical characteristics of fluorescent phthalocyanine dyes; **Pc-1** and **Pc-2** which signal to protons at the red end of the visible spectrum.

References

[1] Tang Ching W, Multilayer organic photovoltaic elements, (Rochester, NY), United States Patent 4164431, 1979.
[2] G. ZGiang, C. C-Hui, F. Z-Qi, H. Wei, Y.S. Kun, C. YChun, D. XGuang, W. Xu, D. Tong, Near-infrared emission from organic light-emitting diodes based on copper phthalocyanine with a periodically arranged Alq$_3$:CuPc/DCM multilayer structure, Chin. Phys. Lett. 25 (2008) 715–718.
[3] C.C. Leznoff, A.B.P. Lever, Phthalocyanines: Properties and Applications, VCH Publications, New York, 1996.
[4] Y. Amao, K. Asai, I. Okura, Fluorescence quenching oxygen sensor using an aluminum phthalocyanine–polystyrene film, Anal. Chim. Acta 407 (1–2) (2000) 41–44.
[5] A.K. Hassan, A.K. Ray, J.R. Travis, Z. Ghassemlooy, M.J. Cook, A. Abass, R.A. Collins, The effect of NO$_2$ on optical absorption in Langmuir–Blodgett films of octa-substituted amphiphilic copper phthalocyanine molecules, Sens. Actuators B-Chem. 49 (1998) 235–239.
[6] F. Baldini, A. Capobianchi, A. Falai, G. Pennesi, A new sandwich-type diphthalocyanine as a potential optical transducer for NO$_2$ detection, Sens. Actuators B-Chem. 51 (1998) 176–180.
[7] J.F. Fernǐandez-Sǐanchez, T. Nezel, R. Steiger, U.E. Spichiger-Keller, Novel optical NO2-selective sensor based on phthalocyaninato-iron(II) incorporated into a nanostructured matrix, Sens. Actuators B-Chem. 113 (2006) 630–638.
[8] J. Spadavecchia, G. Ciccarella, G. Vasapollo, P. Siciliano, R. Rella, UV–vis absorption optosensing materials based on metallophthalocyanines thin films, Sens. Actuators B-Chem. 100 (2004) 135–138.
[9] J. Spadavecchia, G. Ciccarella, P. Siciliano, S. Capone, R. Rella, Spin-coated thin films of metal porphyrin–phthalocyanine blend for an optochemical sensor of alcohol vapours, Sens. Actuators B-Chem. 100 (2004) 88–93.
[10] R. Rella, S. Capone, P. Siciliano, J. Spadavecchia, G. Ciccarella, Spin coated thin films of different metal phthalocyanines and porphyrin-phthalocyanine blend for optochemical sensors of volatile organic compounds, in: Proceedings of SPIE - The International Society for Optical Engineering 5502, 2004, pp. 435–438.

[11] C.J. Liu, W.C. Lu, Optical amine sensor based on metallophthalocyanine, J. Chin. Inst. Chem. Eng. 38 (5–6) (2007) 483–488.

[12] N.E. Koval'skaya, N.A. Kuznetsova, O.L. Kaliya, N.S. Gretsova, I.V. Sokolova, Study of spectral properties of zinc phthalocyanines used as sensitizers in photodynamic therapy, Opt. Spectrosc. 89 (5) (2000) 724–726.

[13] R. Franceschini, G. Iori, L. Polo, G. Bocchiotti, Method of diagnosis and photodynamic therapy of tumours, US Patent, 6,165,441 (2000).

[14] D.B. Papkovsky, G.V. Ponomarev, O.S. Wolfbeis, Longwave luminescent porphyrin probes, Spectrochim. Acta Part A 52 (1996) 1629–1638.

[15] J.N. Miller, M.B. Brown, N.J. Seare, S. Summerfield, in: O.S. Wolfbeis (Ed.), Fluorescence Spectroscopy New Methods and Applications, Springer, Berlin, 1993, p. 189.

[16] F. Yüksel, A.G. Gürek, C. Lebrun, V. Ahsen, Synthesis and solvent effects on the spectroscopic properties of octatosylamido phthalocyanines, New. J. Chem. 29 (2005) 726–732.

[17] S. Derinkuyu, K. Ertekin, O. Oter, S. Denizalti, E. Cetinkaya, Emission based fiber optic pH sensing with Schiff bases bearing dimethylamino groups, Dyes Pigments 76 (2008) 133–141.

[18] N. Kobayashi, H. Ogata, N. Nonaka, E.A. Luk'yanets, Effects of peripheral substitution on the electronic absorption and fluorescence spectra of metal-free and zinc phthalocyanines, Chem.-Eur. J. 9 (2003) 5123–5134.

[19] A.T.R. Williams, S.A. Winfield, J.N. Miller, Relative fluorescence quantum yields using a computer controlled fluorescence spectrometer, Analyst 108 (1983) 1067–1071.

[20] D. Maree, T. Nyokong, K. Suhling, D. Phillips, Effects of axial ligands on the photophysical properties of silicon octaphenoxyphthalocyanine, J. Porphyrins Phthalocyanines 6 (2002) 373–376.

[21] R. Minnes, H. Weitman, H. Lee, S.M. Gorun, B. Ehrenberg, Enhanced acidity, photophysical properties and liposome binding of perfluoroalkylated phthalocyanines lacking C-H bonds, Photochem. Photobiol. 82 (2006) 593–599.